Journal of Biomedical Optics

SPIEDigitalLibrary.org/jbo

Application of Cerenkov radiation generated in plastic optical fibers for therapeutic photon beam dosimetry

Kyoung Won Jang
Takahiro Yagi
Cheol Ho Pyeon
Wook Jae Yoo
Sang Hun Shin
Chiyoung Jeong
Byung Jun Min
Dongho Shin
Tsuyoshi Misawa
Bongsoo Lee

SPIE

Application of Cerenkov radiation generated in plastic optical fibers for therapeutic photon beam dosimetry

Kyoung Won Jang,[a,b] Takahiro Yagi,[a] Cheol Ho Pyeon,[a] Wook Jae Yoo,[b] Sang Hun Shin,[b] Chiyoung Jeong,[c] Byung Jun Min,[c] Dongho Shin,[c] Tsuyoshi Misawa,[a] and Bongsoo Lee[b]
[a]Kyoto University, Research Reactor Institute, Nuclear Engineering Science Division, Asashiro-nishi, Kumatori-cho, Sennan-gun, Osaka 590-0494, Japan
[b]Konkuk University, Research Institute of Biomedical Engineering, School of Biomedical Engineering, Chungju 380-701, Korea
[c]National Cancer Center, Proton Therapy Center, Goyang 410-769, Korea

Abstract. A Cerenkov fiber-optic dosimeter (CFOD) is fabricated using plastic optical fibers to measure Cerenkov radiation induced by a therapeutic photon beam. We measured the Cerenkov radiation generated in optical fibers in various irradiation conditions to evaluate the usability of Cerenkov radiation for a photon beam therapy dosimetry. As a results, the spectral peak of Cerenkov radiation was measured at a wavelength of 515 nm, and the intensity of Cerenkov radiation increased linearly with increasing irradiated length of the optical fiber. Also, the intensity peak of Cerenkov radiation was measured in the irradiation angle range of 30 to 40 deg. In the results of Monte Carlo N-particle transport code simulations, the relationship between fluxes of electrons over Cerenkov threshold energy and energy deposition of a 6 MV photon beam had a nearly linear trend. Finally, percentage depth doses for the 6 MV photon beam could be obtained using the CFOD and the results were compared with those of an ionization chamber. Here, the mean dose difference was about 0.6%. It is anticipated that the novel and simple CFOD can be effectively used for measuring depth doses in radiotherapy dosimetry. [DOI: 10.1117/1.JBO.18.2.027001]

Keywords: Cerenkov radiation; plastic optical fiber; photon beam; dosimeter.

Paper 12691 received Oct. 20, 2012; revised manuscript received Dec. 18, 2012; accepted for publication Dec. 18, 2012; published online Feb. 1, 2013.

1 Introduction

Plastic optical fibers (POFs) have been frequently used as a means of relaying scintillation signals due to the advantages that they offer in radiotherapy dosimetry.[1–3] First, their most favorable capability is remote transmission without significant diminution of the signal. In this process, POFs are relatively immune to environmental influences, including pressure, temperature, humidity, and electromagnetic field.[4] Second, the small radii or thicknesses of POFs make it possible to measure absorbed doses with high-spatial resolution in narrow spaces. Third, POFs made of polymethyl methacrylate (PMMA) or polystyrene (PS) have tissue- or water-equivalent characteristics. Modern radiotherapy dosimetry depends on the accuracy of radiation delivery to a tumor volume. Dosimetric materials should therefore have water-equivalent characteristics to avoid complex conversions arising from material differences between dosimeters and tissues.[5–7] For these reasons, POFs have been used as a component of scintillating fiber-optic dosimeters (SFODs) with water-equivalent organic scintillators for radiotherapy dosimetry.[8–10]

However, the Cerenkov radiation, which is produced by charged particles that pass through a POF, is regarded as a severe noise signal when measuring absorbed doses using a SFOD, because the spectral range of the Cerenkov radiation covers that of the organic scintillator.[11] Moreover, the intensity of Cerenkov radiation depends on incident angles and energies of charged particles, as well as the irradiated lengths of the POF.[12,13] Then, several methods have been developed to remove or correct the Cerenkov radiation generated in a POF.[6,14,15]

Cerenkov radiation is one of the signals induced by interactions between radiations and media, and can be a significant signal in some cases. For therapeutic photon beams, Cerenkov radiation is mainly produced by Compton electrons. Since Compton scattering is the predominating interaction for a photon beam, its depth dose distribution depends on electron fluxes at each depth of a water phantom. In general, the intensity of Cerenkov radiation produced by an electron varies with the velocity of electron relative to light, according to the Frank-Tamm theory. In cases of relativistic electrons, however, the intensity of Cerenkov radiation is nearly independent from velocity or energy of the electron.[16] Therefore, the intensity of Cerenkov radiation is directly proportional to electron fluxes. Consequently, depth doses for a therapeutic photon beam can be obtained by measuring the Cerenkov radiation generated in a POF.

The Cerenkov fiber-optic dosimeter (CFOD) fabricated in this study consists of only POFs and does not employ an organic scintillator. The fabrication procedure is simplified relative to that of a SFOD. Also, the CFOD has enhanced durability for radiation, because the radiation resistance of the POF is much higher than that of an organic scintillator.[17,18] In this study, the Cerenkov radiation induced by a therapeutic photon beam was measured with the use of a POF. In order to characterize the Cerenkov radiation generated in the POF, spectra and intensities of Cerenkov radiation were measured with a

Address all correspondence to: Bongsoo Lee, Konkuk University, Research Institute of Biomedical Engineering, School of Biomedical Engineering, Chungju 380-701, Korea. Tel: +82-43-856-0976; Fax: +82-43-851-0620; E-mail: bslee@kku.ac.kr

0091-3286/2013/$25.00

spectrometer as functions of the irradiated length of the POF and irradiation angle of the photon beam. Also, electron fluxes and total energy depositions of the photon beam were calculated according to water depths using the Monte Carlo *N*-particle transport code (MCNPX). Finally, percentage depth doses (PDDs) of the photon beam were obtained using the CFOD, and the results were compared with those obtained in an ionization chamber.

2 Cerenkov Radiation Generated in Plastic Optical Fiber

When a charged particle travels in a dielectric medium, at a velocity greater than that of light in the same medium, electromagnetic fields close to the particles polarize the medium along their paths, and the electrons in the atoms follow the waveform of the pulse; this is called Cerenkov radiation.[19] The charged particles should have sufficient energies to produce Cerenkov radiation. The Cerenkov threshold energies (CTE; E_{Th}) of charged particles can be calculated using the special theory of relativity as follows[20]

$$E_{\mathrm{Th}} = m_0 c^2 \left(\frac{n}{\sqrt{n^2 - 1}} - 1 \right), \tag{1}$$

where m_0 is the rest mass of a charged particle, c is the speed of light, and n is a refractive index. CTEs of an electron as a function of the refractive index are shown in Fig. 1. The CTEs of the electron to produce Cerenkov radiation in core materials of POFs, including PMMA and PS, are 178 keV and 146 keV, respectively.

The Cerenkov radiation has a cone-shaped propagation with a certain emission angle (θ). The emission angle of Cerenkov radiation can be determined by the refractive index (n) of the medium and the energy (E) of a charged particle as follows[21]

$$\theta = \cos^{-1} \left[\frac{1}{n \sqrt{1 - \frac{1}{\left(\frac{E}{m_0 c^2} + 1 \right)^2}}} \right]. \tag{2}$$

In the case of a therapeutic photon beam, the angle of Cerenkov emission cannot be calculated by Eq. (2) directly, because the Cerenkov radiation is induced by subsequent scattered electrons having various energies. Thus, using the mean energy of Compton electrons over CTE, an approximate emission angle of the Cerenkov radiation can be obtained. The energies of Compton electrons produced in POF with a 1 mm diameter induced by a 6 MV photon beam can be calculated using the MCNPX simulation as shown in Fig. 2; here, the average energy of Compton electrons is about 1 MeV. For this type of electron, the Cerenkov emission angle is about 45 deg in the POF ($n = 1.492$), as shown in Fig. 3. Consequently, since optical fibers have a critical angle to transmit the light signals, the Cerenkov radiation generated in a POF has an angular dependence for the incident beam.

The spectrum of Cerenkov radiation is a continuous spectrum from the ultraviolet (UV) to infrared regions, and its intensity varies with the wavelength (λ). Specifically, the intensity of Cerenkov radiation is inversely proportional to λ^3.[22] Hence, the radiance is stronger in the UV and blue spectral bands than in the infrared.

The intensity of Cerenkov radiation (I_C) generated by a charged particle per unit path can be obtained using the Frank-Tamm formula as[12]

$$I_C = 2\pi\alpha z^2 \frac{d\lambda}{\lambda^2} \left(1 - \frac{1}{\beta^2 n^2} \right), \tag{3}$$

where α is the fine structure constant ($=1/137$), z is the charge of the particle, λ is the wavelength of Cerenkov radiation, n is the refractive index of medium, and β is the velocity of particle relative to light. As seen in Eq. (3), the intensity of Cerenkov radiation is proportional to $(1 - 1/\beta^2 n^2)$. In cases of relativistic electrons, the value of β is close to '1'. And the intensity of Cerenkov radiation is nearly independent from the energies of electrons.[16]

As mentioned above, a major interaction between therapeutic photons and the water phantom is Compton scattering. Thus, the Cerenkov radiation is mainly produced by Compton electrons over CTE. Also, interactions of photons increase linearly for the volume of medium having few millimeter thicknesses. Therefore, the total intensity of Cerenkov radiation generated in the optical fiber can be expressed as

$$\text{total } I_C \propto N_e \pi r^2 l, \tag{4}$$

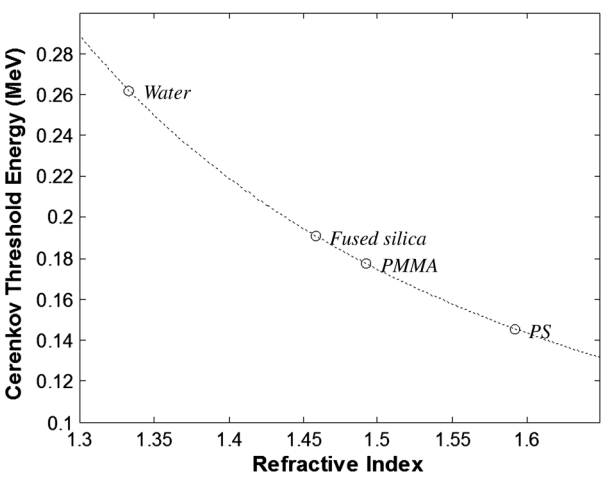

Fig. 1 Cerenkov threshold energies of electrons.

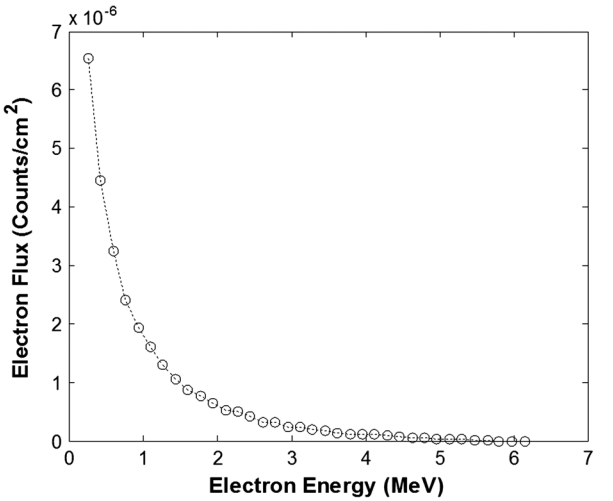

Fig. 2 Calculated energies of Compton electrons produced in the POF induced by 6 MV photon beam using the MCNPX simulation.

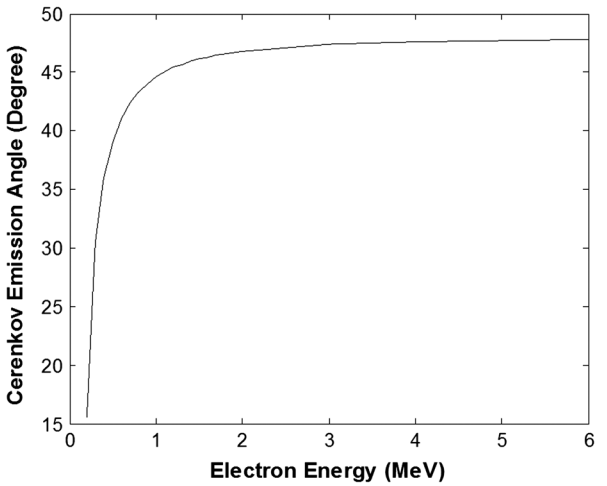

Fig. 3 Emission angle of the Cerenkov radiation generated in the POF according to electron energies.

$$\text{total } I_C = 2\pi^2 r^2 l \alpha z^2 N_e \frac{d\lambda}{\lambda^2}\left(1 - \frac{1}{\beta^2 n^2}\right), \quad (5)$$

where N_e is the number of electrons over CTE per unit volume, r is the radius of optical fiber, and l is the irradiated length of optical fiber.

3 Materials and Methods

Commercial-grade multimode POFs (SH4001, Mitsubishi Co. Ltd., New York) are used to produce and transmit the Cerenkov radiation. The outer diameter of the POF is 1.0 mm and the cladding thickness is 0.01 mm. Refractive indices of the core and the cladding are 1.492 and 1.402, respectively, and the numerical aperture (NA) is 0.510. The NA denotes the light-gathering power, and more light can be guided by a POF with a higher NA. The materials of the core and the cladding are PMMA and fluorinated polymer, respectively. The electron density of PMMA is close to that of water, and it is frequently regarded as a water-equivalent material in a radiotherapy dosimetry. Water-equivalent characteristics of PMMA are listed in Table 1.[23]

The maximum transmission loss of the POF is 0.09 dB/m for the 500 nm collimated light. The transmission characteristic of the POF can be found in Fig. 4. Previous works reported that there is no significant degradation in the light attenuation of the POF up to 15 kilogray (kGy) of irradiation.[18]

A spectrometer (QE65000, Ocean Optics Inc., Dunedin, Florida) is used to measure the spectrum and intensity of Cerenkov radiation. The measurable wavelength range of the spectrometer is between 200 and 925 nm. This type of spectrometer provides about 82% quantum efficiency for a wavelength of

Table 1 Water-equivalent characteristics of PMMA.

Material	Chemical composition	Mass density (g cm^{-3})	Number of electrons per gram (×10^{23})
PMMA	$(C_5O_2H_8)_n$	1.18	3.24
cf. Water	H_2O	1	3.34

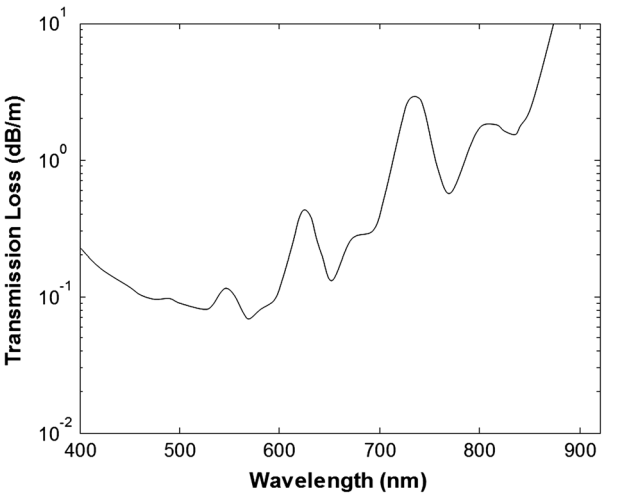

Fig. 4 Transmission characteristic of the POF.

500 nm. The signal-to-noise ratio (SNR) of the spectrometer is 30 dB.

The therapeutic photon beam is provided by a varian clinical linear accelerator (CLINAC) 21EX and its energy and field size are 6 MV and 10×10 cm^2, respectively. The dose rate of the photon beam is 600 MU/min and generally 1 monitor unit (MU) is equivalent to 1 centigray (cGy) for a 10×10 cm^2 beam field at the depth of maximum dose; the CFOD is irradiated for 30 s. To obtain the angular dependence of Cerenkov radiation generated in the POF, the irradiation angle relative to the POF varies from 20 to 90 deg. The source to surface distance (SSD) used in these experiments is 100 cm.

The MCNPX is used to calculate electron fluxes and energy depositions of the 6 MV photon beam in a water phantom. The energy spectrum of the 6 MV photon beam corresponded with that of a previous work.[24] Figure 5 shows the MCNPX simulation scheme. The field size of the photon beam is 10×10 cm^2 and the SSD is 100 cm. Geometrical dimensions of the water phantom used in this simulation are $50 \times 50 \times 50$ cm^3. Here, electron fluxes and energy depositions of the 6 MV photon beam were obtained in the cylinder shaped water cells having same dimensions of the optical fibers.

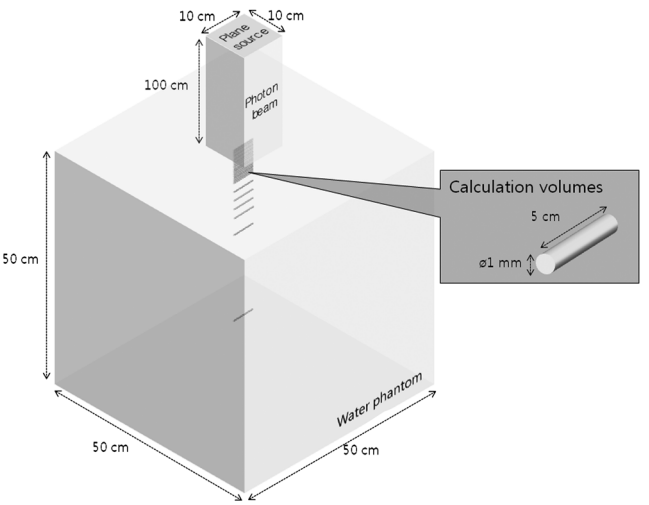

Fig. 5 MCNPX simulation scheme.

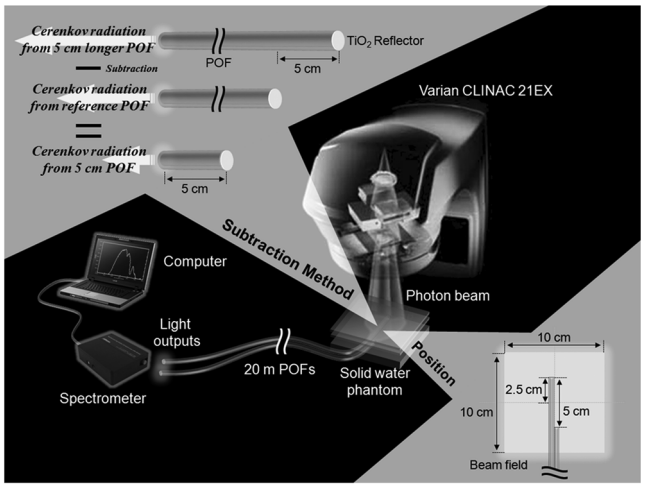

Fig. 6 Subtraction method and experimental setup.

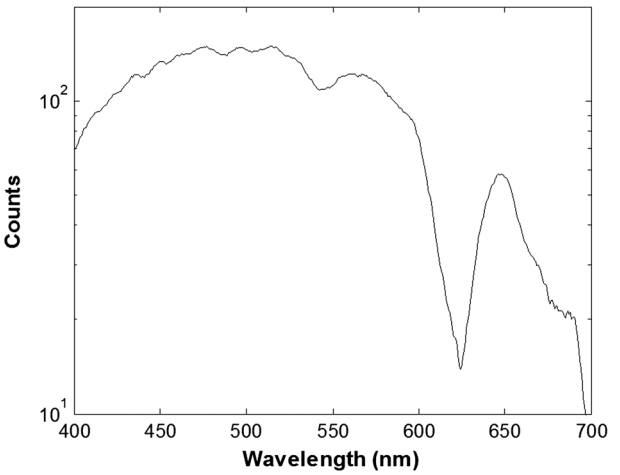

Fig. 7 Spectrum of Cerenkov radiation generated in the POF.

The CFOD for measuring the Cerenkov radiation consists of two POFs having different lengths. A reference POF and 1- to 5-cm longer POFs are used to apply the subtraction method, as shown in Fig. 6. Typically, the subtraction method can be employed for measuring the difference between two sensor signals.[6] In our experiments, the intensity of Cerenkov radiation generated in the limited length of POF is obtained by subtracting the signal of reference POF from that of 1- to 5-cm longer POF. To increase the collection efficiency of Cerenkov radiation, a reflective paint based on TiO_2 is coated at the end of POFs.

The PDDs for the 6 MV photon beam are measured according to depths of a solid water phantom using the CFOD at the center of beam field, as shown in Fig. 6. Generally, the solid water phantom is made of epoxy resins and some powders to control density and radiation properties. When this type of phantom interacts with therapeutic radiations, relative depth doses obtained in solid water phantom are virtually the same as those in liquid water. When the photon beam is irradiated on the CFOD, Cerenkov radiation is transmitted to the spectrometer by 20-m length POFs. Output signals from the spectrometer are measured and displayed with data analysis software (SPECTRA SUITE, Ocean Optics Inc., Dunedin, Florida).

4 Experimental Results and Discussion

4.1 *Measurement of Cerenkov Radiation Generated in Plastic Optical Fiber*

Figure 7 shows the spectrum of Cerenkov radiation generated in the POF. The spectrum was obtained by integrating the counts for 10 s of irradiation. As mentioned above, the Cerenkov radiation has a very broad range of wavelength, and the intensity of Cerenkov radiation increases toward shorter wavelengths.[25]

However, in our measurement, the intensity of Cerenkov radiation has a peak at the wavelength of 515 nm. This discrepancy is caused by the attenuation characteristics of the POF as shown in Fig. 4. In general, the POFs have high-transmission loss in short wavelengths less than 400 nm and have attenuation peaks at wavelengths around 540, 620, and 730 nm. In this experiment, POF with a length of 20 m was used, and thus, the original wavelength of the Cerenkov radiation might be falsified according to the transmission properties of the POF. Typically, POF made of PMMA has minimum attenuation losses at wavelengths of 522, 570, and 650 nm.[26] Since, the intensity of Cerenkov radiation is proportional to λ^{-3}, the integrated data in the wavelength range of 522 ± 20 nm were used throughout this study.

To determine the probe size of the CFOD, the intensity of Cerenkov radiation according to the irradiated length of POF was measured and the results are shown in Fig. 8. In general, the Cerenkov radiation is produced directly by interactions between charged particles and a medium and the intensity of Cerenkov radiation is proportional to the volume of irradiated medium. In Fig. 8, the intensity of Cerenkov radiation increased linearly with an increase of the irradiated length of the POF, because the cross-sectional area of the POF has a uniform value (0.25 mm^2). The Cerenkov radiation generated in the POF is a supersubtle light signal, and therefore a length of 5 cm as the probe size of the CFOD was employed to increase the collection efficiency of Cerenkov radiation. Although this length could cause poor spatial resolution in measuring a planar dose distribution for the beam field, the spatial resolution for the depth dose is only 1 mm according to the diameter of the POF.

Figure 9 shows the calculated relative electron fluxes over CTE and the measured intensities of Cerenkov radiation generated in POF with 5 cm length according to irradiation angles of 6 MV photon beam. For an electron beam, generally, the

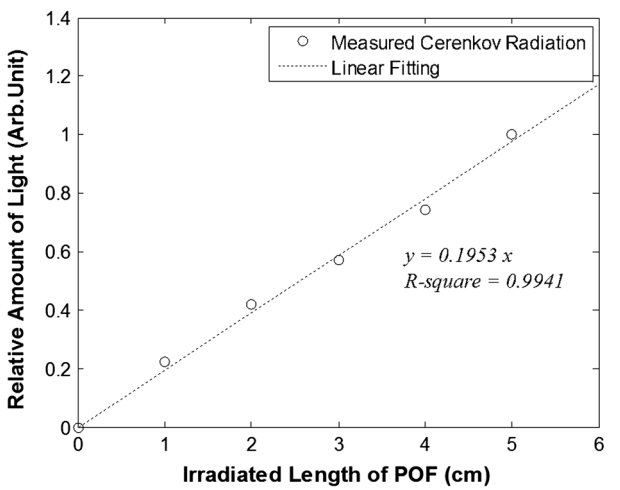

Fig. 8 Intensity of Cerenkov radiation according to the irradiated length of the POF.

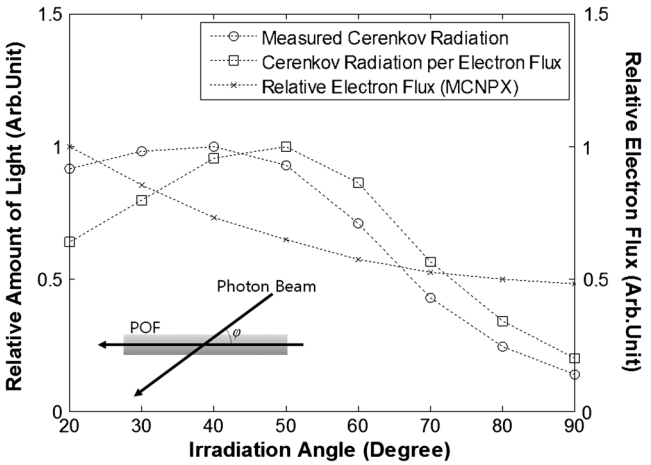

Fig. 9 Electron flux and intensity of Cerenkov radiation according to irradiation angle of the incident photon beam.

intensity of Cerenkov radiation generated in an optical fiber has a peak when the angle (φ) of incident beam is equal to the Cerenkov emission angle (θ).[16] As mentioned in the theoretical section, Cerenkov emission angle is approximately 45 deg when the POF is irradiated by the 6 MV photon beam. However, in our experiment, the intensity peak of Cerenkov radiation was measured in the range of 30 to 40 deg. This difference can be caused by different fluxes of Compton electrons according to irradiation angles of photon beam. In case of the electron beams, the Cerenkov radiation is mainly generated by primary electrons, whereas subsequent electrons produced by Compton scattering are the origin of Cerenkov radiation for the photon beams. Thus, the measured intensities of Cerenkov radiation could be corrected using the fluxes of produced electrons as a function of irradiation angle. In the result, the flux of Compton electron over CTE was obtained using MCNPX simulation and the corrected intensities of Cerenkov radiation have a maximum in the range of 40 to 50 deg as shown in Fig. 9. In the following experiments, to remove the angular dependence of Cerenkov radiation generated in the POF, the irradiation angle is fixed in a perpendicular position relative to the POF.

4.2 *MCNPX Simulations*

Generally, the intensity of Cerenkov radiation is proportional to fluxes of electrons whose energies are over the CTE. In the case of PMMA, the core material of the POF, the CTE of electrons is about 178 keV. Since the primary purpose of this study is to measure the depth doses for a photon beam using the CFOD, the relationship between fluxes of electrons over CTE and energy depositions of the 6 MV photon beam should be determined. Here, electron fluxes and energy depositions of the 6 MV photon beam were calculated according to depths of a water phantom using the MCNPX.

The calculated ratios of electron fluxes over CTE to total electron fluxes according to depths of a water phantom can be found in Fig. 10(a). Here, a saturation value is obtained by averaging the values over 8 mm depth. Throughout this study, we assumed that absorbed doses are proportional to electron fluxes. If the intensities of Cerenkov radiation (electron flux over CTE) are linear to absorbed doses, the ratio of electron flux over CTE to the total electron flux should be uniform. In our simulation, however, the flux ratio of electrons over CTE

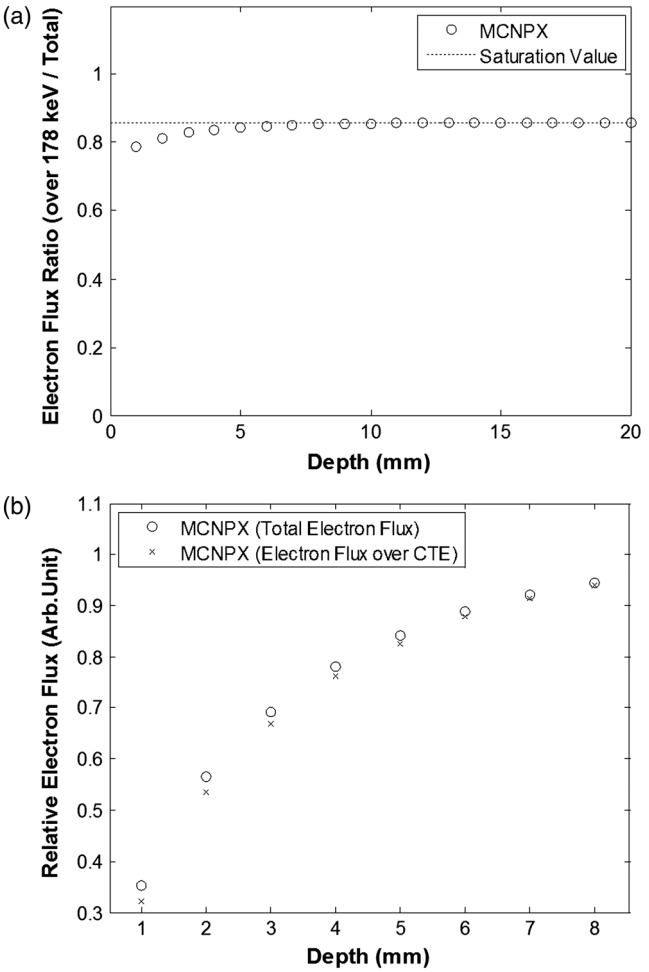

Fig. 10 (a) Calculated ratios of electron fluxes over CTE to total electron fluxes in depths of a water phantom. (b) Relative electron fluxes of total and over CTE below 8 mm depth.

increased gradually until 8 mm depth and then reached the saturation value (0.8578). Calculated total and over CTE electron fluxes below 8 mm depth can be found in Fig. 10(b); here, each electron flux is normalized at the fluxes of 15 mm depth. In this result, as depth increases, the portion of electrons below CTE is decreased.

Typically, energies of the subsequent electrons depend on those of incident photons. Since the therapeutic photon beam generated from the CLINAC consists of bremsstrahlung photons, there are low-energy photons (below 178 keV) in the energy spectrum of the generated photon beam. These types of photons are rapidly attenuated at depths of several millimeters in the medium;[27] here, low-energy electrons are mainly produced by low-energy photons. Therefore, in this region, the ratio of low-energy electrons is higher than that of greater depth. This phenomenon can cause small dose differences in the near-surface region when we measure depth doses for the photon beam using the CFOD because low-energy electrons cannot generate the Cerenkov radiation.

Figure 11 shows the relationship between calculated fluxes of electrons over CTE and energy deposition of the 6 MV photon beam. The results were obtained by one-to-one correspondence of electron fluxes and energy deposition according to water depth. As seen in Fig. 11, the relationship between electron fluxes and energy deposition shows a hysteresis trend. At

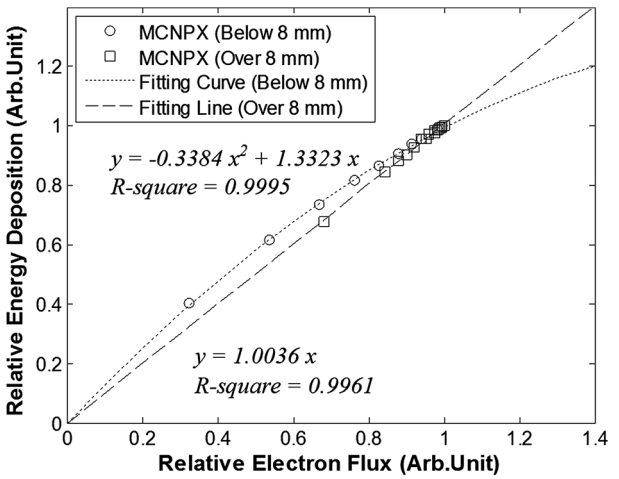

Fig. 11 Relationship between calculated fluxes of electrons over CTE and energy depositions of the 6 MV photon beam.

depths below 8 mm, the energy deposition increased with electron flux according to the polynomial function of the second degree; this is mainly caused by the ratio of electron fluxes over CTE to the total electron fluxes, as shown in Fig. 10. At depths over 8 mm, however, the energy deposition increased linearly according to the near-identity function. Consequently, depth doses for the photon beam are obtainable without any correction using the intensity of Cerenkov radiation over a depth of several millimeters, although some corrections are required in the near-surface region.

4.3 *Measurement of Percentage Depth Doses*

In clinical practice, the central axis dose distribution is characterized by the PDD, which can be defined as the ratio of the absorbed dose at any depth (d_t) to the peak absorbed dose at a fixed reference depth (d_{max}). The PDD can be expressed as:[27]

$$\mathrm{PDD}(\%) = \frac{d_t}{d_{\max}} \times 100. \tag{6}$$

As seen in Eq. (6), the PDD is the ratio of dose at depth to dose at a fixed reference depth, expressed in percentage, and it varies according to SSD, energy, and field size. It has been observed that the typical depth of maximum dosage along the central axis for a 10×10 cm^2 field in a water phantom is about 1.5 cm for a 6 MV photon beam.[27]

Figure 12(a) shows measured PDDs in several millimeters of the solid water phantom using the CFOD. Small dose differences (1.5% to 5.7%) relative to those of the MCNPX can be found in the results. The PDDs obtained with the Cerenkov radiation were corrected using the second-order polynomial function of Fig. 11. The corrected results were in good agreement with those of MCNPX. Although, in this region, the mean difference between the original PDDs obtained with the CFOD and the results of MCNPX was about 3.4%, the difference of the corrected PDDs from the results of the MCNPX was only 0.7%.

The PDD curve for the 6 MV photon beam obtained with Cerenkov radiation generated from the CFOD is presented in Fig. 12(b). Here, corrected results of the CFOD are also employed below 8 mm depth. The PDDs obtained with an ionization chamber are also plotted for comparison with those of

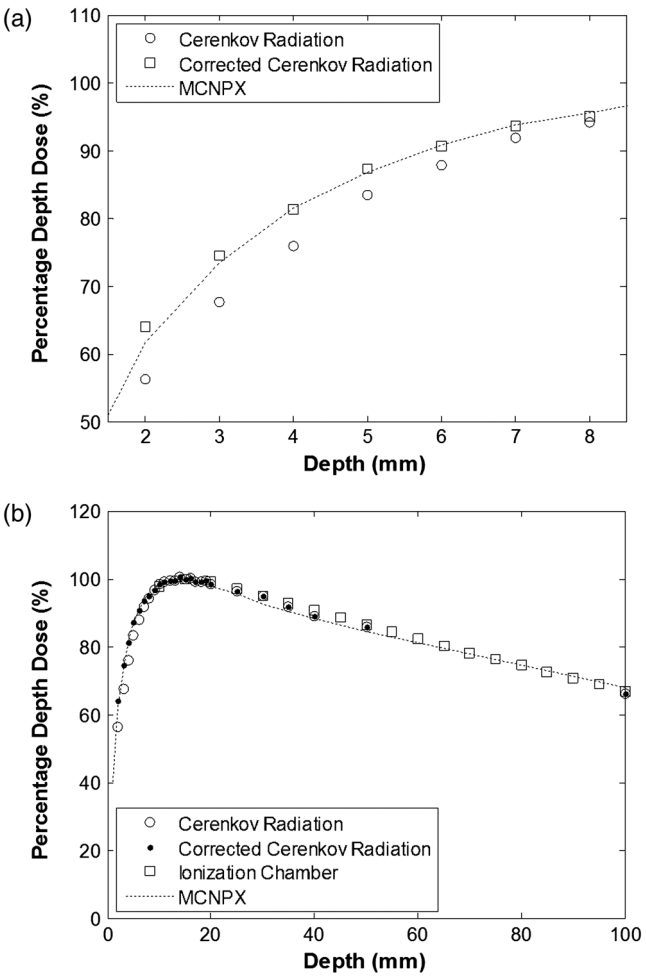

Fig. 12 (a) Measured PDDs in several millimeters (below 8 mm) using the CFOD. (b) Measured PDD curve for the 6 MV photon beam using the CFOD.

the CFOD. The ionization chamber is widely used to measure PDDs in radiotherapy dosimetry because it is the most well proven dosimeter in commercial. In this study, therefore, we used the ionization chamber as a reference dosimeter. As shown in the result, however, we could not measure the PDDs in the region of 0 to 9 mm using the ionization chamber due to its relatively large volume. The obtained PDD curves for the 6 MV photon beam increased steeply according to the depth of d_{max}, and then decreased slowly. The depth of d_{max} obtained by the CFOD, ionization chamber, and MCNPX simulation was 1.5 cm for the 6 MV photon beam. Dose differences between the results of the CFOD and those of the ionization chamber and MCNPX simulation were about 0.6% and 0.7%, respectively.

5 Conclusions

In radiotherapy dosimetry, the Cerenkov radiation generated in a POF is always regarded as a severe noise signal. However, it is also one of the signals produced by interactions between radiation and a medium. In some cases, therefore, the Cerenkov radiation can be a significant signal.

Throughout this study, the CFOD was fabricated without an organic scintillator to measure Cerenkov radiation induced by a therapeutic photon beam. The CFOD consists of only POFs and therefore the fabrication procedure can be simplified relative to

that of the SFOD. In addition, the CFOD has enhanced durability for radiation, because the radiation resistance of POF is much higher than that of an organic scintillator. It was reported that the scintillating fiber and POF can be used for irradiations up to 10 and 15 kGy, respectively.[17,18] Also, at high stopping power such as the Bragg-peaks of heavy charged particle beams, the quenching effect can limit the use of scintillators. On the other hand, the absorbed doses at Bragg-peaks of heavy charged particles can be obtained using the CFOD without quenching effect because the CFOD only consists of POFs without any scintillating material.[28] Moreover, as part of a multi-dimensional dosimeter, the CFOD can be a very useful component relative to the SFOD, because output fluctuations between each dosimeter caused by imperceptibly different lengths of scintillators and dislocations between scintillators and POFs can be removed.

In this study, the Cerenkov radiation induced by a therapeutic photon beam was measured using POF. To characterize the Cerenkov radiation generated in the POF, spectra and intensities of Cerenkov radiation were measured with a spectrometer as functions of the irradiated length of the POF and irradiation angle of the photon beam. The intensity of Cerenkov radiation generated in the POF increased linearly with increasing irradiated length of the POF, and the spectral peak of Cerenkov radiation was measured at a wavelength of 515 nm due to the transmission properties of the POF. Also, the intensity peak of Cerenkov radiation was measured in the irradiation angle range of 30 to 40 deg.

Based on MCNPX simulations, the relationship between fluxes of electrons over CTE and energy deposition of a 6 MV photon beam could be determined. At depths below 8 mm, the energy deposition increased with increasing electron fluxes according to the second-order polynomial function. At depths over 8 mm, however, the energy deposition increased linearly according to a near-identity function.

Finally, the PDDs for the 6 MV photon beam were obtained using the CFOD and the results were compared with those of an ionization chamber. The PDDs for the photon beam could be obtained using the CFOD over a depth of 8 mm without any correction, although some corrections were required in the near-surface region. Mean dose differences between the results of the CFOD and those of the ionization chamber and MCNPX simulation were about 0.6% and 0.7%, respectively.

Future studies will be carried out to compensate the defects of CFOD by shortening the dosimeter probe for planar dose measurements with higher spatial resolution and to develop a correction method for the near-surface region. It is anticipated that the novel and simple CFOD for measuring Cerenkov radiation can be effectively used for measuring depth doses in radiotherapy dosimetry.

Acknowledgments

This work was supported by JSPS KANKENHI Grant Number 24F09E02076, and this work was supported by the National Research Foundation of Korea (NRF) Grant funded by the Korean government (MEST) (No. 2012029724). Also this paper resulted from the Konkuk University research support program.

References

1. L. Archambault et al., "Water-equivalent dosimeter array for small-field external beam radiotherapy," *Med. Phys.* **34**(5), 1583–1592 (2007).
2. F. Lacroix et al., "Clinical prototype of a plastic water-equivalent scintillating fiber dosimeter array for QA applications," *Med. Phys.* **35**(8), 3682–3690 (2008).
3. B. Lee et al., "Measurement of two-dimensional photon beam distributions using a fiber-optic radiation sensor for small field radiation therapy," *IEEE Trans. Nucl. Sci.* **55**(5), 2632–2636 (2008).
4. B. Lee, W. Y. Choi, and J. K. Walker, "Polymer-polymer miscibility study for plastic gradient index optical fiber," *Polymer Eng. Sci.* **40**(9), 1996–1999 (2000).
5. K. H. Becks et al., "A multichannel dosimeter based on scintillating fibers for medical applications," *Nucl. Instrum. Meth. A* **454**(1), 147–151 (2000).
6. A. S. Beddar et al., "A miniature "Scintillator-Fiberoptic-PMT" detector system for the dosimetry of small fields in stereotactic radiosurgery," *IEEE Trans. Nucl. Sci.* **48**(3), 924–928 (2001).
7. A. S. Beddar, "Plastic scintillation dosimetry and its application to radiotherapy," *Radiat. Meas.* **41**(Suppl. 1), S124–S133 (2007).
8. G. Bartesaghi et al., "A scintillating fiber dosimeter for radiotherapy," *Nucl. Instrum. Meth. A* **581**(1), 80–83 (2007).
9. K. W. Jang et al., "Fabrication and optimization of a fiber-optic radiation sensor for proton beam dosimetry," *Nucl. Instrum. Meth. Phys. Res. A* **652**(1), 841–845 (2011).
10. B. Lee et al., "Characterization of one-dimensional fiber-optic scintillating detectors for electron-beam therapy dosimetry," *IEEE Trans. Nucl. Sci.* **55**(5), 2627–2631 (2008).
11. A. M. Frelin et al., "Spectral discrimination of Cerenkov radiation in scintillating dosimeters," *Med. Phys.* **32**(9), 3000–3006 (2005).
12. B. Brichard et al., "Fiber-optic gamma-flux monitoring in a fission reactor by means of Cerenkov radiation," *Meas. Sci. Technol.* **18**(10), 3257–3262 (2007).
13. S. H. Law et al., "Transmission of Cerenkov radiation in optical fibers," *Opt. Lett.* **32**(10), 1205–1207 (2007).
14. M. A. Clift, P. N. Johnston, and D. V. Webb, "A temporal method of avoiding the Cerenkov radiation generated in organic scintillator dosimeters by pulsed mega-voltage electron and photon beams," *Phys. Med. Biol.* **47**(8), 1421–1433 (2002).
15. M. A. Clift, R. A. Sutton, and D. V. Webb, "Dealing with Cerenkov radiation generated in organic scintillator dosimeters by bremsstrahlung beams," *Phys. Med. Biol.* **45**(5), 1165–1182 (2000).
16. A. S. Beddar, T. R. Mackie, and F. H. Attix, "Cerenkov light generated in optical fibres and other light pipes irradiated by electron beams," *Phys. Med. Biol.* **37**(4), 925–935 (1992).
17. H. Blumenfeld, M. Bourdinaud, and A. V. Stirling, "Ageing of scintillating fibers, natural and otherwise," *Nucl. Instrum. Meth. A* **279**(1–2), 281–284 (1989).
18. Y. M. Protopopov and V. G. Vasil'chenko, "Radiation damage in plastic scintillators and optical fibers," *Nucl. Instrum. Meth. Phys. Res. B* **95**(4), 496–500 (1995).
19. J. V. Jelly, "Cerenkov radiation and its applications," *J. Appl. Phys.* **6**(7), 227–232 (1955).
20. Z. W. Bell and L. A. Boatner, "Neutron detection via the Cherenkov effect," *IEEE Trans. Nucl. Sci.* **57**(6), 3800–3806 (2010).
21. G. F. Knoll, *Radiation Detection and Measurement*, pp. 711–713, John Wiley & Sons, New York (1999).
22. J. Lambert et al., "Cerenkov light spectrum in an optical fiber exposed to a photon or electron radiation therapy beam," *Appl. Opt.* **48**(18), 3362–3367 (2009).
23. F. M. Khan, *The Physics of Radiation Therapy*, Williams & Wilkins, Baltimore (1994).
24. D. Sheikh-Bagheri and D. W. O. Rogers, "Monte Carlo calculation of nine megavoltage photon beam spectra using the BEAM code," *Med. Phys.* **29**(3), 391–402 (2002).
25. S. F. De Boer, A. S. Beddar, and J. A. Rawlinson, "Optical filtering and spectral measurements of radiation induced light in plastic scintillation dosimetry," *Phys. Med. Biol.* **38**(7), 945–958 (1993).
26. J. Zubia and J. Arrue, "Plastic optical fibers: an introduction to their technological processes and applications," *Opt. Fiber Technol.* **7**(2), 101–140 (2001).
27. W. R. Hendee, G. S. Ibbott, and E. G. Hendee, *Radiation Therapy Physics*, p. 131, John Wiley & Sons, New York (2005).
28. K. W. Jang et al., "Fiber-optic Cerenkov radiation sensor for proton therapy dosimetry," *Opt. Express* **20**(13), 13907–13904 (2012).